



Estimating shear stress from moving boat acoustic Doppler velocity measurements in a large gravel bed river

Louise C. Sime,¹ Robert I. Ferguson,² and Michael Church³

Received 29 March 2006; revised 9 October 2006; accepted 31 October 2006; published 15 March 2007.

[1] Moving boat acoustic Doppler current profiling (ADCP) is increasingly used to measure discharge in large rivers. We investigate whether useful information about bed shear stress can be recovered from such data. Alternative ways to estimate local bed shear stress using the logarithmic law of the wall and spatial averaging are tested using ADCP transects across lower Fraser River, Canada. Repeatability is assessed by comparing estimates from outward and return boat tracks. The most precise method uses the vertically averaged mean velocity and a zero-velocity height based on bed grain size information. The accuracy of the assumed zero-velocity height can be judged by consistency between estimates using mean velocity and near-bed velocity. Shear stress estimates from unconstrained log-law fits are less repeatable and tend to overpredict, and mean shear stress estimates using the depth-slope product are unreliable in this river because of nonuniform flow.

Citation: Sime, L. C., R. I. Ferguson, and M. Church (2007), Estimating shear stress from moving boat acoustic Doppler velocity measurements in a large gravel bed river, *Water Resour. Res.*, 43, W03418, doi:10.1029/2006WR005069.

1. Introduction and Aims

[2] Gravel bed rivers normally have a pronounced bar-pool-riffle morphology over which there is considerable spatial variation in flow depth (h), vertically averaged mean velocity (U), and local bed shear stress (τ). This hydraulic diversity is important for in-stream ecology and is responsible for the divergence in bed load flux that creates and modifies the morphology through local erosion, deposition, and sediment sorting. Until recently it was impractical to gain a detailed knowledge of the velocity and shear stress fields in such rivers because available current meters yielded only single-point measurements, restricting data collection to a few tens of points in each of several cross sections [e.g., Hickin, 1978]. However, the advent of acoustic Doppler current profilers (ADCP hereafter, without implying any specific instrument or manufacturer) now allows rapid measurement of large numbers of vertical profiles of near-instantaneous velocity from a stationary or moving boat. Over the last two decades ADCP technology has developed from being a novel tool for laboratory applications to a viable method of measuring velocity fields in rivers. Doppler profiling is increasingly standard for operational stream gauging [e.g., Yorke and Oberg, 2002], is starting to be used in research on flow structures and habitat in large rivers [e.g., Kostaschuk *et al.*, 2005; Shields and Rigby, 2005; Ellis and Church, 2005; Dinehart and Burau, 2005], and is potentially useful for validation of CFD simulations.

[3] Our purpose in this paper is to investigate whether useful information on local and cross-section average shear stress can be recovered from typical moving boat ADCP

measurements made for stream-gauging purposes. Such measurements are by far the commonest type of ADCP deployment. They consist of a large number of near-instantaneous velocity profiles closely spaced across the channel. The individual profiles are highly irregular because of turbulent fluctuations and instrument noise, but the discharge calculation has high precision because it integrates a large number of profiles and the errors are averaged out [Muste *et al.*, 2004]. Data of this type are not ideal for estimating local velocities or shear stresses at particular positions, for which repeat profiling from a stationary boat [e.g., Kostaschuk *et al.*, 2005] is preferable since that averages the turbulent fluctuations. Nonetheless, moving boat profiling has the advantage of continuous coverage over long transects, and data obtained in this way are becoming widely available. We therefore considered it useful to explore how best to extract local hydraulic information from routine data of this type and to assess the reliability of the results. We do this using typical stream-gauging ADCP measurements made in 1999 at a series of transects across Lower Fraser River in British Columbia. As is usual, the data include replicate ADCP traverses of each transect. We take advantage of this to assess the precision of alternative ways of estimating local shear stress by examining how repeatable the results are for replicate traverses. Absolute accuracy is harder to assess since no other measurements were made in 1999 from which we can make independent estimates of local shear stress, but we investigate the mutual consistency of alternative ADCP-based methods and discuss how transect averages of ADCP-based estimates compare with the traditional estimate of mean shear stress from the depth-slope product.

2. Study Reach, Field Data, and Initial Data Processing

[4] The ADCP data were collected in Lower Fraser River, British Columbia, between 97 and 136 km from the sea

¹British Antarctic Survey, Cambridge, UK.

²Department of Geography, Durham University, Durham, UK.

³Department of Geography, University of British Columbia, Vancouver, British Columbia, Canada.

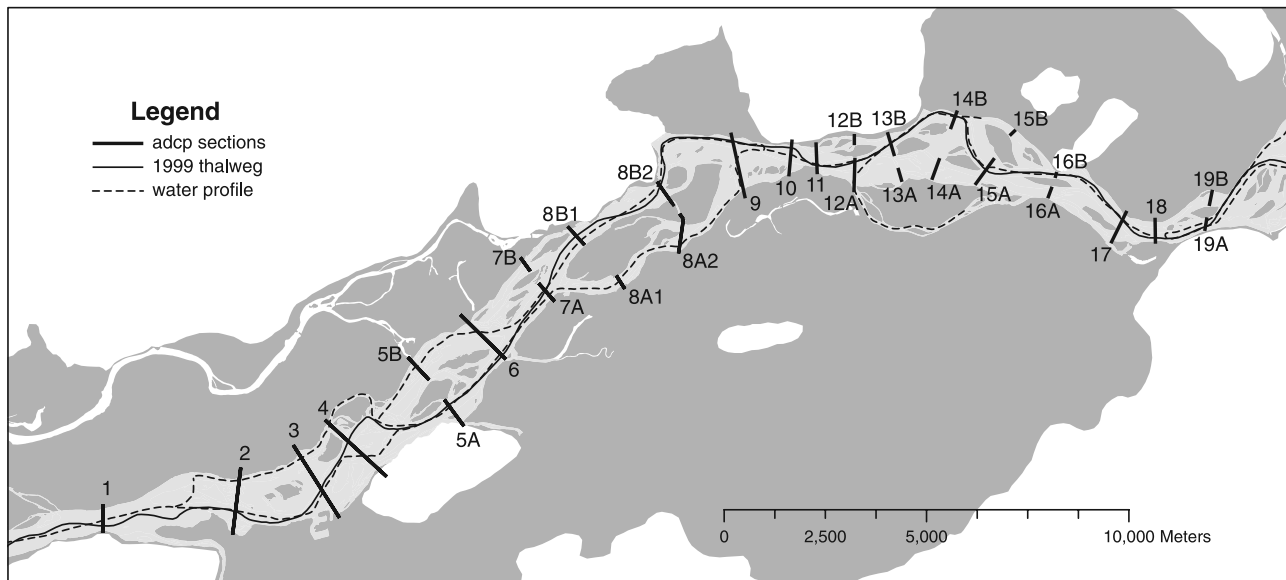


Figure 1. Map of study reach of Lower Fraser River showing the main channel talweg, lines of ADCP transects, and tracks of water surface profiles. Light gray, dark gray, and white areas are the active channel zone, vegetated islands and floodplains, and bedrock, respectively.

(Figure 1). The lowest few kilometers of the reach are in the gravel-sand transition but above km 102 the river has a gravel bed and is mildly braided around bars and vegetated islands (see *McLean et al.* [1999] for further details). Detailed bathymetric and hydraulic surveys of the reach were commissioned from the Hydrographic Services Unit of Public Works and Government Services Canada in 1999 as part of a study of sedimentation and river stability. The hydraulic survey had two components: velocity profiling from a moving boat across main and branch channels, and water surface profiling along the main channel and some branches. The ADCP transects are numbered in upstream sequence in Figure 1 using A and B for left and right channels in divided reaches. The long-term mean discharge and mean annual flood at the top of the reach are $2800 \text{ m}^3 \text{ s}^{-1}$ and $8800 \text{ m}^3 \text{ s}^{-1}$, to which about 10% is added by Harrison River which enters just below transect 9. The hydraulic survey was made over eight days of high but gradually falling stage in early August. Discharges at the times of measurement were about 8800, 8300, 7900, 6100, and $5900 \text{ m}^3 \text{ s}^{-1}$ for transects 1–4, 5–7, 8.1–9, 10–15, and 16–19 respectively. Much of the bed is mobile at these discharges.

[5] The gravel bars exposed in winter low flows are compound features and often have distal avalanche faces up to 2–3 m high with sand in the lee, but bar tops are planar with no small-scale bed forms apart from thin ($\sim 0.1 \text{ m}$) and loosely packed gravel sheets. Pebble counts made in 2000–2001 at upper and mid bar locations show gradual downstream fining along the reach (Figure 2) but there is considerable local variation, some of it in the form of down- and cross-bar fining but some seemingly random. Little is known about the bed in deeper parts of the river. A 1983 dredge sample from the talweg near transect 1 had a bimodal sand/gravel distribution with $D_{84} = 20 \text{ mm}$. Sonar traces and underwater video between km 122 and 127 indicate grain sizes no coarser than on adjacent bars but a strongly imbricated bed with grain structures of amplitude

0.1–0.2 m (C. Perrin, personal communication, 2002). A rock sill plunges into the channel close to transect 16B, and the right bank at 8B2 is a rock cliff.

[6] The principles and practice of ADCP velocity measurement in rivers are described by *Yorke and Oberg* [2002], *Muste et al.* [2004], *Kostaschuk et al.* [2005], and *Shields and Rigby* [2005]. The 1999 Fraser River data were collected using a 600 kHz four-beam ADCP made by RD Instruments (RDI), with positioning from a Trimble 4000DS RTK GPS receiver with nominal horizontal precision of 2 m. Single-ping ensembles were collected every 1 s, giving a mean spacing of 1–1.5 m along each transect. Ensembles consist of east-north-vertical velocity components for 0.5-m bins starting 1.4 m below the surface. The 1.4-m blanking distance means that less than half the cross-section area is measured in four particularly shallow branch channels (transects 7B, 12B, 15B, 19B) none of which conveys more than 8% of river discharge; these transects are excluded hereafter. Measurements could not be made in water shallower than about 2 m so the transects do not cover bar margins and gently sloping banks. During the ADCP survey every line was repeated in the reverse direction, keeping as close to the outward track line as possible. Boat movement was subtracted using the dGPS record since bottom tracking gives erroneous results when the bed is mobile [*Rennie et al.*, 2002]. The ADCP survey did not include echo sounder depth measurements so we used the median of the depths indicated by the four ADCP beams. These depths refer to widely separated locations and often differ by several decimeters, leading to uncertainty in the inferred bed elevation for each profile. Sidelobe interference and bed load movement can bias velocity measurements near the bed, and the fourth beam of the RDI instrument showed greater uncertainty near the bed. Before analysing the data any bin within 0.25 m of the estimated bed level was discarded, along with all bins with a current speed that was implausibly high ($>8 \text{ m s}^{-1}$) or below the uncertainty from the fourth beam.

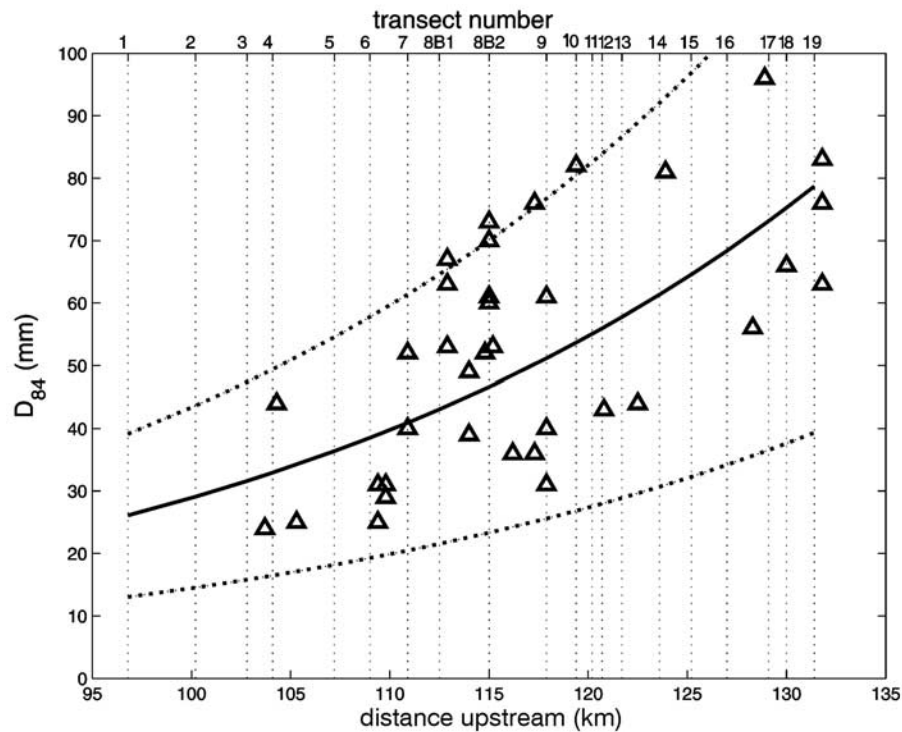


Figure 2. Downstream trend and local variation in surface grain size at upper and mid bar locations exposed at low discharge. D_{84} denotes diameter that 84% of pebbles are finer than, established by grid count. Sample values are shown by triangles, and transect locations are shown by vertical dotted lines. Solid line is exponential trend fitted to data, and dashed lines show a $\pm 50\%$ envelope.

[7] Water surface profiles were surveyed on the same days as the ADCP measurements using kinematic GPS along curving tracks along the main talweg and branch channels (Figure 1). The measurement spacing depends on boat speed; it was generally 35–40 m between transects 7 and 18 but 20–25 m elsewhere. Elevations have an absolute accuracy of ± 0.2 m but appear to be locally much more precise than that since 95% of changes in elevation from one point to the next are smaller than 0.05 m. Profiles surveyed on different days were corrected by PWGSC for changes in river level and could therefore be amalgamated, using interpolation for one short gap under a bridge near transect 18. We estimated local water surface slope from the main channel profile by computing a running regression of elevation on track distance, using 13 or 21 points according to measurement spacing to give a near-constant smoothing window of 0.4–0.5 km. The standard error of a smoothed slope value is generally less than ± 0.00004 , so steep slopes are estimated with higher precision than gentle ones. Any deviation of boat track from the direction of steepest slope will lead to underestimation of the true slope, but this cosine error is only a few per cent for even a 15° – 20° deviation.

3. Theory and Analytical Methods

[8] In this section we review briefly the available range of general approaches for estimating local shear stress, explain our choice, discuss in detail the ways in which we implemented it, and outline how we assessed the precision and accuracy of alternative methods.

3.1. Estimation of Shear Stress

[9] Methods for estimating local bed shear stress (τ) in gravel bed rivers and practical issues in applying different methods have been discussed by several authors, including *Whiting and Dietrich* [1991], *Ferguson and Ashworth* [1992], *Wilcock* [1996], *Biron et al.* [1998, 2004], and *Smart* [1999]. They can be grouped into methods using turbulence statistics, a quadratic stress assumption, or the logarithmic law of the wall.

[10] The first approach analyses high-frequency measurements of 3-D velocity components to estimate the skin friction component of τ from the Reynolds stress [e.g., *Heathershaw*, 1979; *Stacey et al.*, 1999; *Biron et al.*, 2004] or total kinetic energy [e.g., *Stapleton and Huntley*, 1995; *Biron et al.*, 2004]. This requires long time series (several minutes at a point) so is not possible with moving boat deployments.

[11] The quadratic-stress approach estimates τ as $\rho C_d U^2$ where ρ is water density and C_d is an appropriate drag coefficient for the local bed configuration. This method is sometimes used to estimate the form component of shear stress over dunes, where C_d scales with bed form steepness [e.g., *Kostaschuk et al.*, 2004]. The problem in applying it to rough plane bed conditions, as in our study reach, is that there is no agreed constant value of C_d . One variant of the third approach implicitly estimates C_d from relative submergence, and a closely related approach is adopted in 2-D hydrodynamic and morphodynamic models that assume a spatially uniform value of Manning's n [e.g., *Nicholas*, 2003].

[12] The third approach, adopted here, is to estimate local shear stress from the vertical gradient of current speed u at height z above the bed on the assumption that part or all of the profile follows the logarithmic “law of the wall”

$$\frac{u}{u_*} = \frac{1}{\kappa} \ln\left(\frac{z}{z_0}\right) \quad (1)$$

[13] Here $u_* = (\tau/\rho)^{0.5}$ is the shear velocity, $\kappa \approx 0.4$ is von Karman’s constant, and z_0 is the small positive height at which $u = 0$. For well-sorted uniformly packed sediment $z_0 \approx D_{50}/30$ where D_{50} is the median grain size. The log law is often a good approximation throughout the flow depth in gravel bed rivers [e.g., *Ferro and Baiamonte*, 1994; *Smart*, 1999] but departures from it can occur up to a few grain diameters above the bed [e.g., *Wiberg and Smith*, 1991; *Nikora et al.*, 2004] and also in the upper half or more of the flow if secondary currents are present [e.g., *Bridge and Jarvis*, 1977]. In our study reach bed effects should not extend above ~ 0.5 m. Secondary circulation may be appreciable at transects 7A (just below a confluence) and 8B2 (exit of a bend) but not elsewhere in view of low sinuosity and high width/depth ratios.

[14] Equation (1) can be utilized in several ways. If the time-averaged velocity has been measured at several different heights, $u = a + b \ln(z)$ can be fitted by ordinary least squares regression yielding estimates of u_* as κb and z_0 as $\exp(-a/b)$. We use τ_{LF} to denote a bed shear stress estimate by this log-law fitting procedure. The precision of the method depends on the number of velocity measurements used, how accurately they represent the time-averaged velocity, and how accurately the bed level is known. Most moving boat ADCP data, including those from Fraser River, are problematic in the second and third respects so some form of averaging is desirable to combine information from adjacent verticals and thus reduce the effect of individual errors; we discuss this below. If a time-averaged velocity profile is available, uncertainty about the effective zero height can also be reduced by trying a range of zero-plane displacements and selecting the one that gives the best fit of the log law to the profile. We tried this on subsets of our data but found that it seldom gave an optimum for any displaced bed level between the maximum and minimum depths indicated by the four ADCP beams. This failure appears to be a consequence of the considerable scatter in the near-instantaneous profiles obtained by moving boat ADCP.

[15] Shear stresses can also be estimated from a single u , z pair within the valid height range of (1) if z_0 is known or assumed. *Wilcock* [1996] considered two variants, one using a single near-bed measurement to obtain an estimate which we denote by τ_{u1} and the other using the vertically averaged mean velocity U to obtain an estimate which we denote by τ_U . *Wilcock* treated U as occurring at height h/e , as it does if the log law holds over the full depth. We note that this is implicitly a quadratic stress method since, from (1), it amounts to

$$\tau_U = \rho C_d U^2 \quad (2a)$$

$$C_d = \kappa^2 / \ln^2(h/ez_0) \quad (2b)$$

where the drag coefficient is seen to depend weakly on relative submergence. The skin friction equations of *Yalin* [1992] and *van Rijn* [1984] that were used by *Kostaschuk et al.* [2004] to partition stress over a dune field are also of this form, while the constant- n modeling approach implies $C_d = gn^2/h^{1/3}$ which like (2b) is a weak inverse dependence on depth. *Wilcock* found by analysing replicate profiles at the same points during steady flow that precision improved from τ_{LF} to τ_{u1} to τ_U . His result is for time-averaged velocities at a particular set of measurement heights at a single site, and does not necessarily apply to instantaneous ADCP velocities at a different spacing in a different river. He also calculated that to get the same average values of τ by each method z_0 had to be set at $0.095D_{90}$. This agrees with previous findings of $z_0 \approx 0.1D_{84}$ in profiles that match the log law closely [*Whiting and Dietrich*, 1991; *Ferguson and Ashworth*, 1992].

[16] In analyzing the Fraser River ADCP data we computed the three estimates τ_{LF} , τ_{u1} , and τ_U for each ensemble of each transect, but modified *Wilcock*’s methods slightly to suit the different situation. Correlations between u and $\ln(z)$ for the near-instantaneous ensembles in the ADCP data are inevitably lower than for time-averaged profiles; they are typically 0.6–0.8, and at best >0.9 , but a small proportion in slow flowing zones at one or other end of a transect are negative and were excluded from the τ_{LF} calculation. In calculating τ_U we treated U as occurring at the mean height of the ADCP bins used to compute it; this is usually less than h/e because there are no measurements from the top 1.4 m of the flow. As well as computing τ_{u1} using a single velocity at $0.25 \text{ m} < z < 0.75 \text{ m}$ in each ensemble, we calculated a second bottom velocity estimate of shear stress (denoted by τ_{u2}) using the average of the two or three bins below 1.5 m.

[17] We also followed *Wilcock* and previous workers in assuming $z_0 = 0.1D_{84}$ for the estimates τ_{u1} , τ_{u2} , and τ_U . To apply this we had to decide how best to make use of the grain size data shown in Figure 2. It might seem logical to use the D_{84} measurement nearest to each ADCP transect, but this is unreliable given the degree of local streamwise variance apparent in Figure 2 and the likelihood of additional lateral variance not picked up by the bar top sampling. Using the mean D_{84} for the nearest bar would reduce this problem, but some transects are over 2 km from the nearest exposed bar. We considered it more robust to use a trend value which makes use of all the data and allows quantification of uncertainty in the assumed value of z_0 at each transect. The exponential fit shown in Figure 2 gives a reduction in D_{84} from 82 to 27 mm between transects 19 and 1. D_{84} at particular locations departs from the trend by up to $\pm 50\%$ but transect averages are likely to show less scatter, and we show later that the ensuing uncertainty in τ_{u1} and τ_U is smaller still. However, if the true ratio of z_0 to D_{84} differs from 0.1, for example because of imbricated clast structures, our assumption will lead to systematic bias in estimates of shear stress.

3.2. Averaging Methods and Assessment of Precision

[18] All estimates of τ from individual ADCP profiles are subject to uncertainty introduced by turbulent fluctuations in velocity, sidelobe interference, imprecise knowledge of the exact bed elevation, and general instrument noise. *Muste et al.* [2004] found that instantaneous profiles at fixed

locations in rivers deviated by up to about $\pm 20\%$ from the long-term mean profile. In similar tests in Fraser River in 2004 we found the standard deviation of instantaneous current speed at most heights was about 10–20% of the time-average speed, but over 30% in the bottom 0.25 m. As noted by *Muste et al.* [2004] averaging helps reduce this imprecision; for example, the mean of 10 instantaneous values each with a 15% standard deviation will have a standard error of only 5%. Some ADCP campaigns targeted specifically to local hydraulics have taken advantage of this principle. *Kostaschuk et al.* [2004] used spatial averaging from a slowly moving boat to estimate the mean velocity profile over a dune field, and *Dinehart and Burau* [2005] used three-ping ensemble averaging followed by spatial averaging to quantify small cross-stream velocities which would otherwise be swamped by noise.

[19] In analyzing the 1999 Fraser River data we compared two methods of spatial averaging which we term “fit then average” (f-t-a) and “aggregate then fit” (a-t-f). The f-t-a approach involves making individual estimates of u^* for each ensemble, applying moving window averaging of the u^* values for this ensemble and all others within a specified radius, then converting the mean u^* to τ . The a-t-f approach aggregates all ensembles within a specified radius and fits a single log law to each overlapping set of measurements. When calculating τ_{u1} using a-t-f we used the mean of the lowest velocity measurement in each ensemble within the set, rather than the single lowest point. We compared f-t-a and a-t-f for five different averaging radii from 1.25 m to 20 m, equivalent to averaging anything between a few ensembles and several tens of ensembles.

[20] The out-and-back replication of the ADCP transects allows assessment of the repeatability of shear stress estimates by different combinations of estimator and smoothing method. We computed smoothed estimates of τ_{LF} , τ_U , and τ_{u1} within each averaging radius of every point on each outward transect, first using f-t-a smoothing then using a-t-f smoothing, to give six sets of estimates for each transect. We then located all points on the return track that were within the same radius of each point on the outward track and computed the equivalent six sets of replicate estimates for the same locations. This comparison is only possible where the return track deviated little from the outward track, but by pooling results from different transects we have a sample size of >1000 at the smallest radius and >10,000 at the largest radius. The greater the precision of any particular combination of estimation method and averaging method, the closer the agreement should be between the outward track and return track estimates of shear stress. We used the product moment correlation coefficient to quantify strength of agreement and inspected the correlation plots for any evidence of bias.

3.3. Assessing the Accuracy of ADCP Estimates of Shear Stress

[21] The discharge that is estimated from a moving boat ADCP survey is essentially a linear function of a large number of individually noisy velocity measurements, so the good agreement between discharges obtained using ADCP and more traditional methods implies there is no systematic bias in ADCP velocity measurements. It is nevertheless possible that ADCP-based estimates of local shear stress

using the log law are biased because they combine the noisy data in a nonlinear way, or because of error in the assumed z_0 for the τ_U , τ_{u1} , and τ_{u2} methods. No fixed boat measurements were made in 1999 and we have no other means of obtaining independent estimates of local shear stress at that time for direct comparison with our ADCP-based estimates. Less direct assessments of accuracy are nevertheless possible using the transect-averaged values $\langle \tau_{LF} \rangle$, $\langle \tau_U \rangle$, $\langle \tau_{u1} \rangle$, and $\langle \tau_{u2} \rangle$ obtained by using the log law and ADCP data in different ways.

[22] We use correlation plots of one method against another, with points for each transect, to check the mutual consistency of different methods. Any systematic deviation from the 1:1 line would suggest one method is biased relative to the other, whereas 1:1 agreement would suggest both methods are accurate or both are biased by the same amount. The methods using mean or bottom velocity and an assumed z_0 are liable to bias if the $z_0 = 0.1D_{84}$ assumption is inappropriate or our bar top values of D_{84} are unrepresentative of deeper parts of the river. Underestimation of the true z_0 would lead to underestimation of shear stress. However, the sensitivity of the estimators τ_U , τ_{u1} , and τ_{u2} to error in assumed z_0 is not the same, and this opens the possibility that 1:1 consistency can be equated with accuracy. Each estimator is of the form

$$\tau = \rho \kappa^2 u^2 / x^2 \quad (3)$$

where $x = \ln(z/z_0)$ and z_0 is the assumed (not true) value. The sensitivity of τ to z_0 is therefore

$$\frac{\partial \tau}{\partial z_0} = \frac{\partial \tau}{\partial x} \frac{\partial x}{\partial z_0} = \frac{2}{x} \frac{\tau}{z_0} \quad (4)$$

or in relative terms

$$\frac{\delta \tau}{\tau} = \frac{2}{\ln(z/z_0)} \frac{\delta z_0}{z_0} \quad (5)$$

Thus a given percentage change in z_0 creates a smaller percentage change in τ as z/z_0 increases. On a given transect τ_{u1} , τ_{u2} , and τ_U use the same value of z_0 but progressively larger values of z : 0.25–0.75 m, 0.75–1 m, and anything up to 10 m. Thus τ_{u1} is most sensitive to error in z_0 and τ_U least sensitive. Substituting average values $z = 0.5$ m, 0.88 m, and 3 m into equation (5) shows that a 50% increase in the assumed z_0 from an initial choice of 0.005 m would increase the τ_{u1} , τ_{u2} , and τ_U estimates by 22%, 19%, and 16% respectively. In the ideal situation of full depth logarithmic profiles and no measurement error, exact coincidence of the three estimates is therefore possible only if the assumed z_0 is correct; otherwise the estimates must differ, more so the further the assumed z_0 is from the true value. The difference in sensitivity is small and will be swamped by measurement error at the scale of individual ensembles or local spatial averages, but it should be detectable in transect averages based on a large number of ensembles. A systematic difference between, say, $\langle \tau_{u1} \rangle$ and $\langle \tau_U \rangle$ could then be interpreted as showing that we have the wrong value of z_0 whereas 1:1 agreement would suggest we have the right value and both $\langle \tau_{u1} \rangle$ and $\langle \tau_U \rangle$ are accurate. The same

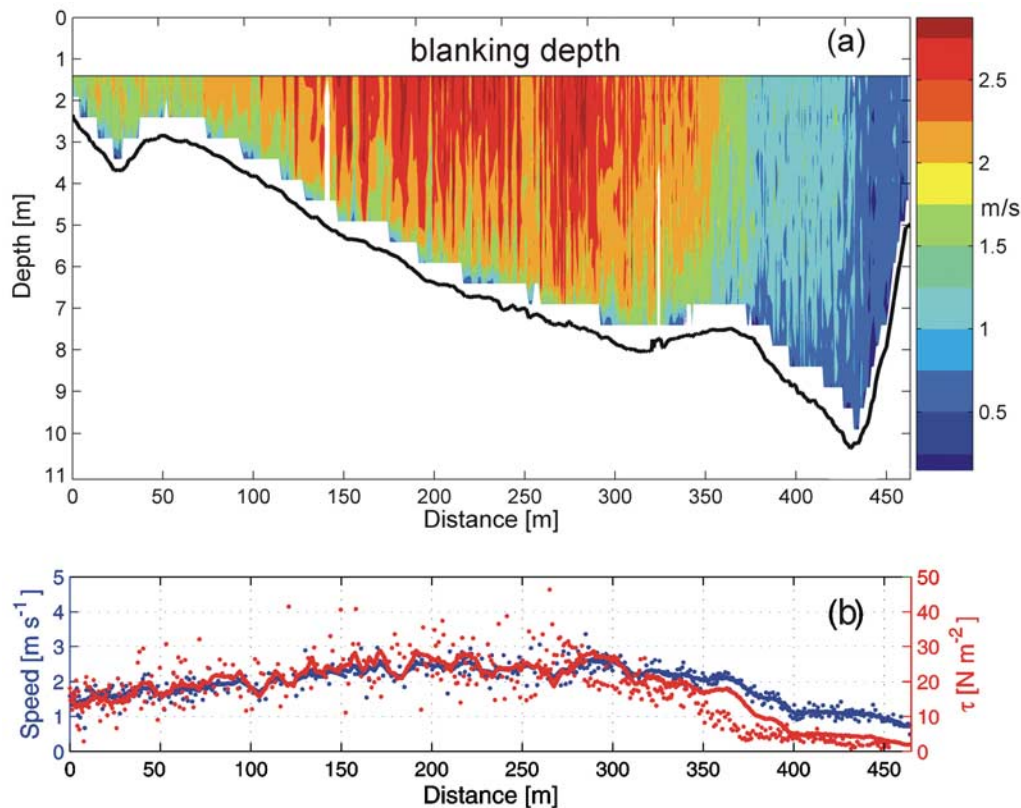


Figure 3. Example of raw ADCP measurements and derived data for transect 10. (a) Current speeds in m s^{-1} after deleting near-bed and other doubtful values but without further processing. (b) U and τ_U for individual ensembles (dots) and smoothed values (curves) using 5-m fit-then-average processing.

numerical example also indicates the sensitivity of τ_{u1} and τ_U to uncertainty in D_{84} , and shows that the $\pm 50\%$ envelope around the scatter in Figure 2 translates to only about a 20% uncertainty in shear stress in this river.

[23] The other comparison we make is between transect-averaged ADCP-derived shear stresses and the standard uniform flow equation for reach-averaged shear stress:

$$\langle \tau_0 \rangle = \rho g \langle h \rangle S \quad (6)$$

where $\langle h \rangle$ is the transect-averaged water depth derived from the ADCP data and S the water surface slope at the intersection with each ADCP transect, derived from the water surface profiling described above. Equation (6) is derived from the momentum balance in uniform flow, in which the water surface slope is the same as the mean bed slope and is constant along the channel. This is a significant simplification of the generally nonuniform flow conditions in lower Fraser River, but the full gradually varied flow momentum equation cannot be used to estimate the energy slope between successive ADCP transects because they span different proportions of channel width and convey different discharges. Equation (6) is not therefore a reliable test of the accuracy of our ADCP-based methods, but the comparison is interesting because $\langle \tau_0 \rangle$ is widely used. We make the comparison using correlation plots, and also by calculating what local energy slope would be necessary in (6) for $\langle \tau_U \rangle$ to match $\langle \tau_0 \rangle$ at each transect then comparing

these values with the observed downstream variation of water surface slope.

4. Results

[24] The general nature of the raw ADCP data and of some of the products of our data-processing algorithms is illustrated for a representative transect in Figure 3. Figure 3a demonstrates three typical features: there is substantial local variability in the raw data; both depth and velocity vary laterally and thus by implication so does local shear stress; and the highest velocities and velocity gradients are often not in the deepest part of the channel but on the flank of a gravel bar. In this example the talweg is the downstream continuation of the slough channel of a bar 1 km upstream. Figure 3b shows how the depth-averaged velocity U , and the τ_U shear stress estimate derived from it, vary across the transect. As might be expected the patterns of lateral variation in U and τ_U are similar, but they are not identical: note for example the lower shear stresses for a given velocity in the deepest part of the section.

4.1. Precision of Alternative Shear Stress Estimators

[25] The extent to which estimates of local shear stress are repeatable using outward and return ADCP tracks depends on the way the log law is used, the averaging radius, and whether averaging is done before or after fitting the log law. This repeatability is a measure of the precision of each method, with a higher repeatability correlation indicating a more precise method. Figure 4 shows the

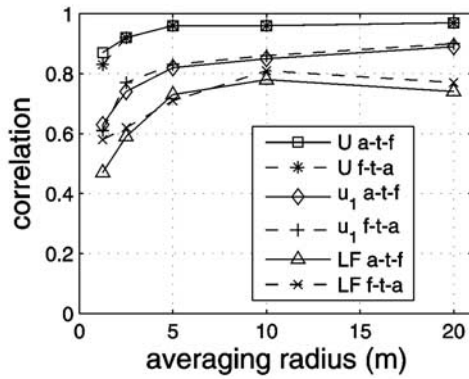


Figure 4. Correlation between estimates of local shear stress on outward and return ADCP tracks using different averaging radii, estimation methods (LF, U, and u1; see text for details), and averaging methods (a-t-f and f-t-a; see text). Correlations are for all possible locations on all transects.

results for each combination of these three factors when information from all transects is combined. The first obvious pattern in this plot is that increasing the averaging radius to at least 5 m improves the precision of every combination of fitting and averaging methods. Increasing the radius beyond 5 m gives no further improvement for τ_U and only a slight improvement for the other methods. The second message of Figure 4 is that for any given averaging radius, τ_U is more precise than τ_{u1} which in turn is more precise than τ_{LF} . This is the same pattern as *Wilcock* [1996] found. Finally, neither the aggregate correlations nor correlations for individual transects show a systematic difference in precision between the aggregate-then-fit and fit-then-average methods over the range of radii we tested. With a 5-m averaging radius the f-t-a smoothing gives slightly

better precision and we use this combination in the rest of the paper.

[26] The repeatability tests are illustrated in more detail in Figure 5. This shows the outward/return correlation plots for each estimation method using a 5-m averaging radius. The points mostly lie fairly close to the 1:1 line, indicating that return-track estimates of shear stress do generally resemble outward track estimates. Occasional “whiskers” running away from the general diagonal trend in the τ_U plots (and also present in the other plots but hidden by general scatter) indicate local discrepancies between outward and return track estimates because of peculiarities in one ensemble that affect several adjacent points in the plot because of the overlapping averaging windows. The estimated shear stresses extend to much higher (and implausible) values for the fitting method in which z_0 is estimated from the data (τ_{LF}) than when using a D_{84} -based roughness height (τ_U and τ_{u1}). This casts doubt on the reliability of the unconstrained fit; we discuss possible sources of unreliability later. Finally, as was apparent in Figure 4, the precision of τ_U is clearly superior to that of τ_{LF} or τ_{u1} , with less scatter and a higher correlation coefficient. When individual transects are considered, τ_U performs better than either alternative at all but two transects and its outward/return correlation exceeds 0.9 at all but three. This suggests that estimating shear stress from vertically averaged velocity and D_{84} is a robust method that works in a reproducible way in a variety of conditions. The other estimators give much more variable results, with correlations dropping below 0.5 for some transects.

[27] The same differences in repeatability are apparent when transect-averaged values of estimated shear stress are considered. Exact agreement between $\langle \tau \rangle$ from outward and return tracks is not expected because boat tracks inevitably differed, sometimes substantially. This is reflected in differ-

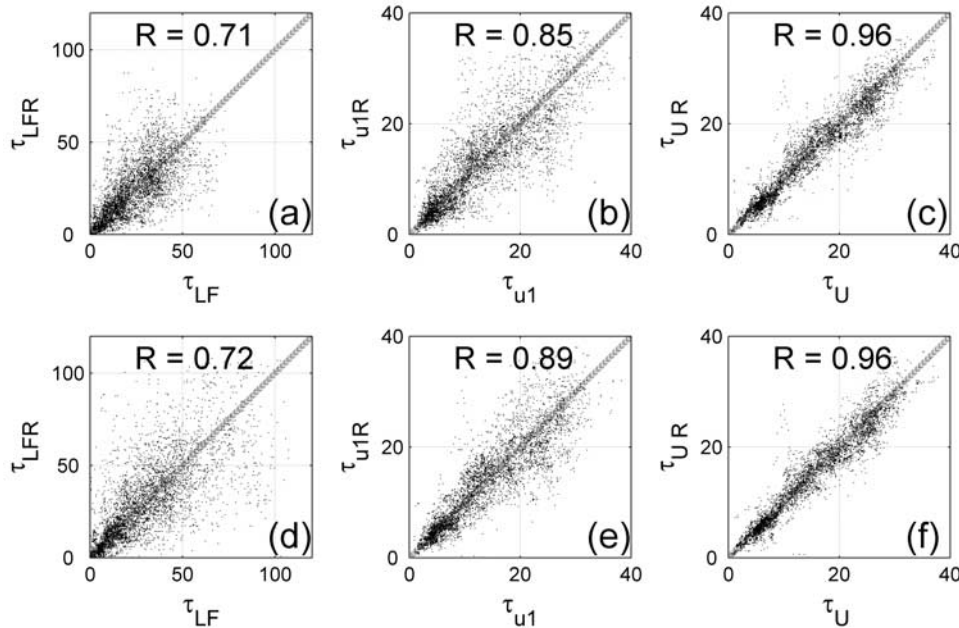


Figure 5. Correlation plots of shear stress estimates by the LF, u1, and U methods for the same locations from outward and return boat tracks. Each plot combines data from all transects. (a–c) Average-then-fit smoothing and (d–f) fit-then-average smoothing (see text for details).

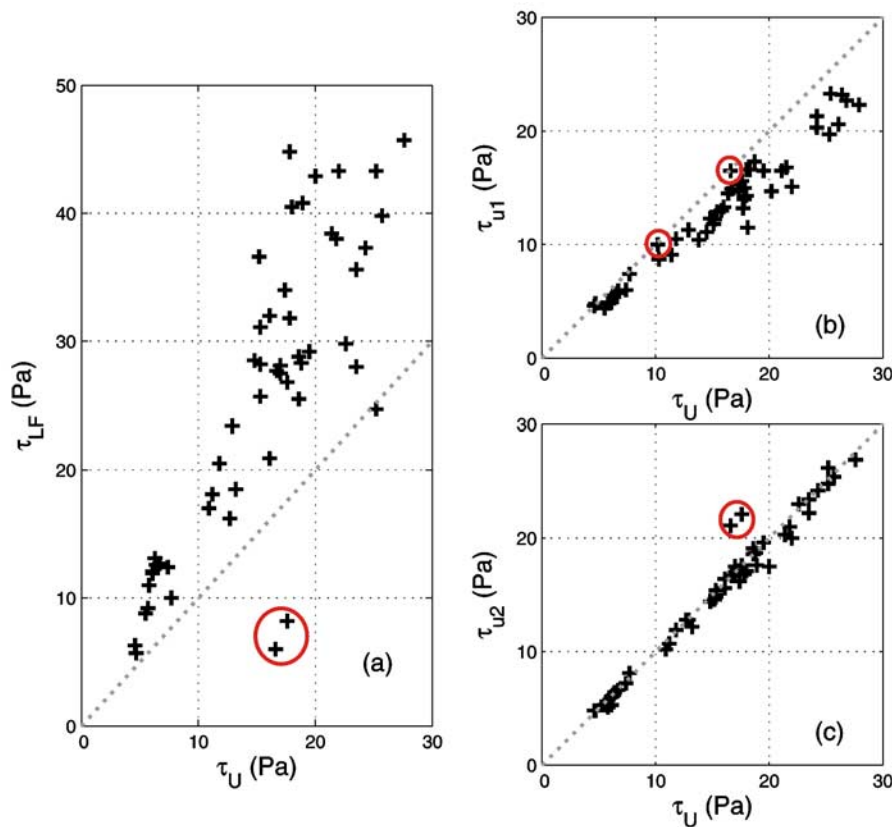


Figure 6. Correlation plots of transect-averaged shear stress estimated by alternative ways of using the log law. Each data point represents the out or back estimate for one of the transects in the location map of Figure 1. Circled outliers are discussed in text.

ences in mean depth $\langle h \rangle$ of up to 19% with a median difference of 8%, and in mean current speed $\langle U \rangle$ of up to 25% with a median of 5%. Estimates of $\langle \tau \rangle$ by the U and u2 methods were as repeatable as $\langle U \rangle$ itself, with median differences of only 4–5%. $\langle \tau_{u1} \rangle$ was slightly less repeatable, with median and maximum differences of 10% and 49%, and $\langle \tau_{LF} \rangle$ was still more erratic with median and maximum differences of 28% and 46%.

4.2. Consistency and Accuracy of Alternative Estimators of Shear Stress

[28] Any systematic difference between transect-averaged shear stresses obtained using the LF, U, u1 and u2 methods indicates bias in one or more method. Broad agreement between $\langle \tau \rangle$ estimated by two methods need not mean either is accurate, but we noted in section 3.3 that close agreement between the U and u1 (or u2) methods might be used to argue that both are accurate since the main source of error in both methods is uncertainty about z_0 and the estimators differ in their sensitivity to z_0 .

[29] Correlation plots of $\langle \tau \rangle$ using different pairs of methods are shown in Figure 6. The data set is reduced slightly to increase the validity of these comparisons. Any ensemble which fails our quality control tests for τ_{LF} or τ_{u1} is not used for τ_U or τ_{u2} either, and two wide but mostly shallow transects (13A and 14A) are omitted. Over 60% of ensembles in these transects are shallower than 3 m so that τ_U is based on only a few more bins than τ_{u2} . The

remaining 26 transects have only 0–37% of ensembles shallower than 3 m, so τ_U is largely independent of τ_{u2} .

[30] Figure 6 shows that $\langle \tau_{LF} \rangle$ is quite weakly correlated with $\langle \tau_U \rangle$ ($r = 0.81$) but $\langle \tau_{u1} \rangle$, $\langle \tau_{u2} \rangle$ and $\langle \tau_U \rangle$ are very strongly intercorrelated ($r \geq 0.98$). Each plot has two outliers, all representing the same transect (16B). The anomalous results for this transect may be related to two peculiarities: the north side of the river here flows partly on rock and is unusually deep and fast, and the ADCP error velocities are also high so that far more near-bed bins than at any other transect were rejected in our quality control. Apart from this site the trends in Figure 6 are clear. The transect averages based on free fitting of the log law ($\langle \tau_{LF} \rangle$, Figure 6a) are usually considerably higher than those based on the mean velocity and assumed z_0 ($\langle \tau_U \rangle$), by about 70% on average and over 100% at some transects. The estimates by the lowest-bin method ($\langle \tau_{u1} \rangle$, Figure 6b) are systematically lower than $\langle \tau_U \rangle$ by an average of 15% (Figure 6b) but those using all bins below 1.5 m ($\langle \tau_{u2} \rangle$, Figure 6c) agree closely with $\langle \tau_U \rangle$, with all but the 16B points close to the 1:1 line and a mean and median difference of only 1%. The three correlation plots amongst $\langle \tau_{LF} \rangle$, $\langle \tau_{u1} \rangle$, and $\langle \tau_{u2} \rangle$ are not shown since their nature is apparent from Figures 6a–6c: $\langle \tau_{u1} \rangle$ and $\langle \tau_{u2} \rangle$ are very highly correlated but differ by 14% on average, and $\langle \tau_{LF} \rangle$ is generally far higher than $\langle \tau_{u1} \rangle$ or $\langle \tau_{u2} \rangle$.

[31] The almost 1:1 agreement in Figure 6c between $\langle \tau_U \rangle$ and $\langle \tau_{u2} \rangle$, despite their different sensitivity to error in z_0 ,

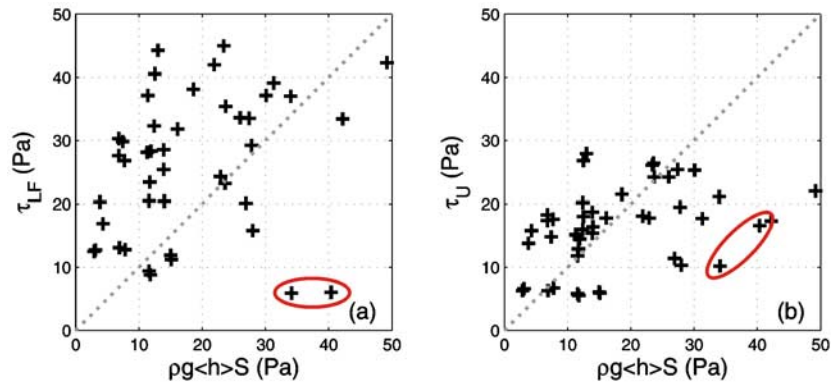


Figure 7. Correlation plots of transect-averaged shear stresses estimated from ADCP measurements using (a) free fit of log law and (b) mean velocity and assumed z_0 , plotted against estimates from the depth-slope product.

can be used to argue that our z_0 values are about right on average, both τ_U and τ_{u2} are approximately unbiased, and the scatter about the trend reflects local departures from the assumed smooth downriver trend in z_0 . However, this argument cannot be accepted without an explanation for why Figure 6b does not also show a 1:1 relation between $\langle\tau_U\rangle$ and $\langle\tau_{u1}\rangle$. Had $\langle\tau_{u1}\rangle$ and $\langle\tau_{u2}\rangle$ been in 1:1 agreement but $\langle\tau_U\rangle$ systematically different, the explanation could have been a widespread departure from logarithmic profiles in the upper part of the flow. However, the results do not show this pattern, and we noted earlier that only two transects are likely to have appreciable secondary circulation. What could cause τ_{u1} to be systematically lower than τ_{u2} is widespread departure from a logarithmic profile in a near-bed roughness layer affected by clast wakes [e.g., *Wiberg and Smith, 1991; Nikora et al., 2004*]. We also note that τ_{u1} is inherently less reliable than τ_U and τ_{u2} since it is based on a single velocity per ensemble instead of several. If $\langle\tau_U\rangle$ and $\langle\tau_{u2}\rangle$ are unbiased, the implication of Figures 6b and 6a is that $\langle\tau_{u1}\rangle$ is moderately biased and $\langle\tau_{LF}\rangle$ is heavily biased.

[32] Figure 7 compares the replicate ADCP-based estimates of transect-averaged shear stress using the free fit and mean velocity methods ($\langle\tau_{LF}\rangle$ and $\langle\tau_U\rangle$) with $\langle\tau_0\rangle$ calcu-

lated from the depth-slope product using equation (3). The slope used to calculate $\langle\tau_0\rangle$ is the smoothed value nearest the intersection of the water surface profile with the ADCP transect. This is not available for some of the smaller branch channels so fewer transects are plotted in Figure 7 than Figure 6. The correlations are very weak (0.2 for $\langle\tau_{LF}\rangle$, 0.4 for $\langle\tau_U\rangle$) and transect 16B (ringed in the plots) is anomalous again. In most cases $\langle\tau_{LF}\rangle$ greatly exceeds $\langle\tau_0\rangle$, by about a factor of two on average. The discrepancy between $\langle\tau_U\rangle$ and $\langle\tau_0\rangle$ is less systematic, with a median difference of only 10% but a very large (factor of 3) scatter. This scatter is far more than the $\pm 20\%$ or so that could be attributed to uncertainty in D_{84} if $z_0 = 0.1D_{84}$ is in fact the appropriate scaling.

[33] We suggested in section 3.3 that a uniform flow calculation of $\langle\tau_0\rangle$ is likely to be unreliable in a river with pronounced bar-pool-riffle morphology. This doubt is reinforced by Figure 8 which shows that water surface slope is highly variable along the main channel in the reach. There is an overall downstream decline but the most striking feature is an irregularly cyclic pattern with a wavelength of 1–2 km and an amplitude that often exceeds $\pm 50\%$ of the local trend value. This cyclicity has too long a wavelength to be an artifact of single rogue GPS elevations, and far too large an

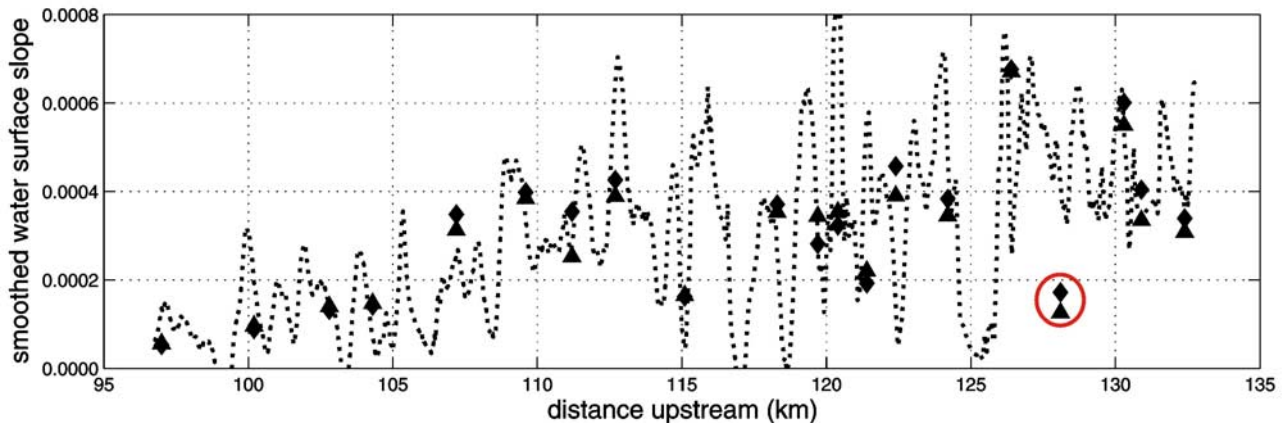


Figure 8. Variation of smoothed water surface slope (dashed line) along the main channel in the study reach. The solid symbols mark the locations of the ADCP transects; their vertical plotting position is explained in the text.

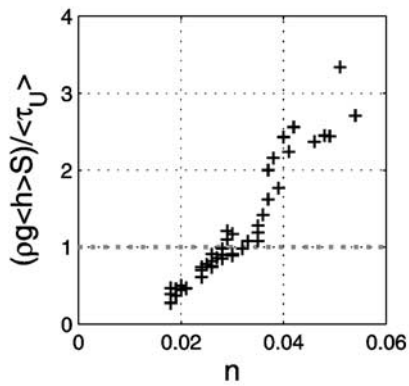


Figure 9. Scatterplot showing how the discrepancy between transect-averaged shear stresses estimated from the depth-slope product and from ADCP measurements is related to Manning's n as estimated using water surface slope.

amplitude to be explained by differences between boat track and direction of steepest slope. It reflects instead the pronounced riffle-pool variation which persists in this river even in flood conditions. The minima near km 117 and km 125 reflect the backwater effect of major diagonal bar complexes that span the river, and at km 117 force the main flow round a headland. The graph makes clear that water surface slope is far from constant past most of the ADCP transects, suggesting the likelihood of drawdown/backwater and acceleration/deceleration effects which are not allowed for in equation (6). A further complication is that the water surface slope could vary laterally in some transects because flow is diverging over a bar head or crossing a diagonal riffle.

[34] Figure 8 also includes a second comparison between ADCP estimates and the depth-slope product. This is to calculate what uniform flow slope would be required in (6) to make $\langle\tau_0\rangle$ match $\langle\tau_U\rangle$ at each transect, and see how these slope values compare with the measured water surface slopes in the vicinity of each transect. The results of this calculation are shown by the solid symbols in Figure 8, two for each transect since the replicate ADCP traverses are plotted separately. Many of them deviate substantially from the measured slope at the exact distance of the transect intersection, as was shown by the scatter in Figure 7b, but almost all of them are within the range of water surface slope encountered by going a short distance up or downstream from each transect. They also show a general downstream reduction that is compatible with the general downstream trend in measured slope. The most obvious anomaly is again transect 16B (ringed points in Figure 8) where the required uniform flow slope plots well below the curve of measured slope, indicating that a uniform flow calculation of $\langle\tau_0\rangle$ using any slope in the vicinity would exceed $\langle\tau_U\rangle$.

[35] As a check on the depth-slope estimates of mean shear stress we calculated transect-averaged values of Manning's roughness coefficient $n = \langle h \rangle^{2/3} S^{1/2} / \langle U \rangle$ using the local water surface slope from Figure 8 and the mean depth and velocity from the outward and return ADCP traverses at each transect. The n values have a plausible mean of 0.031 but range below 0.02 at some transects and

above 0.05 at others. Figure 9 shows that the transects with unusually low or high n values are also those with the biggest discrepancies between ADCP-based and depth-slope estimates of mean shear stress. The range of n values is far wider than could be explained by differences in D_{84} or $\langle h \rangle / D_{84}$ and there is no clear downstream trend in the values. The estimates of $\langle h \rangle$ and $\langle U \rangle$ are quite precise since they are averaged across large numbers of ensembles, and there is no reason to think they are systematically biased, so we infer that anomalously low or high values of n either reflect uncertainties in the slope used in the calculation or identify localities where departure from flow uniformity makes it inappropriate to use Manning's equation or equation (6). This reinforces our skepticism about the reliability of the depth-slope estimates in a river such as this.

5. Discussion

[36] The results in section 4.1 and Figures 4 and 5 show it is possible to obtain repeatable estimates of local shear stress in a large gravel bed river from moving boat ADCP measurements. Precision is greatest when local shear stress is estimated from the vertically averaged mean velocity in each profile using the logarithmic law of the wall and a roughness height estimated from bed grain size information. This is essentially the same method as *Wilcock* [1996] recommended for estimating local shear stress from single velocity profiles obtained using traditional current meters in smaller rivers. The main difference is that moving boat ADCP measurements need some spatial averaging to smooth turbulent fluctuations. Good repeatability, and by implication high precision, required averaging over a 5–10 m radius in our study, i.e., over about ten ensembles. Averaging can be done by fitting the log law then averaging over several adjacent ensembles, or by aggregating several ensembles and then fitting the log law, with little difference in repeatability. In principle, moving boat ADCP measurements made specifically to map patterns of velocity and shear stress could be done with a ping rate, boat speed, and ensemble averaging that gave repeatable estimates without need for further smoothing. This merits further investigation, though we note that our approach in which averaging is part of the postprocessing of the measurements gives more user control, and that averaging over a fixed radius gives a uniform spatial window whereas averaging a fixed number of pings does not.

[37] The inferior precision of the τ_{LF} method in which z_0 as well as u^* is estimated from the data is probably due to the sensitivity of the unconstrained log-law fit to measurement error in bed elevation and near-bed velocity. This is a problem even with hand-held single-point current meters [*Ferguson and Ashworth*, 1992; *Biron et al.*, 1998] and is accentuated when using moving boat ADCP because of relatively higher turbulence intensity near the bed, sidelobe interference, the effect of bed load movement, and the greater difficulty of estimating the exact bed elevation. The results in section 4.2 and Figure 6 suggest that estimates of shear stress using this method are on average too high. This bias may be due to the nonlinearity of the log law. The upward bias in u^* in the event of an unrepresentatively low near-bed velocity or incorrectly low bed elevation exceeds the downward bias in the reverse situations, and the percentage bias is then doubled when u^* is

squared to obtain τ , leading to a skewed distribution of error. Use of an echo sounder to obtain a more precise bed elevation would reduce one of the sources of uncertainty and bias with this method.

[38] The methods which use the log law with a prespecified value of z_0 avoid some of these uncertainties, but the τ_{u1} method using a single near-bed velocity is still vulnerable to the effects of turbulence and uncertainty in bed elevation, and is reproducible only through averaging of adjacent ensembles. The τ_{u2} method using the two or three bins within 1.5 m of the bed is less sensitive to these problems, and the τ_U method using the vertically averaged velocity has still greater inherent smoothing and is least sensitive to uncertainty in bed elevation. It is therefore not surprising that τ_U gave the most repeatable results. The accuracy of these methods evidently depends on the accuracy of the assumed z_0 , and is hard to assess with much confidence in the absence of reliable independent evidence, but we take the almost 1:1 agreement between $\langle\tau_{u2}\rangle$ and $\langle\tau_U\rangle$ despite their differential sensitivity to z_0 as circumstantial evidence that both of these methods are accurate and our $z_0 = 0.1D_{84}$ assumption is a valid generalization for the reach as a whole. If so, $\langle\tau_{u1}\rangle$ is biased by about 15% on average. On the basis of these results, and also on the more intuitive grounds that it involves more averaging of the noisy data than other methods, we suggest that τ_U is probably the most accurate as well as most precise way to estimate shear stress from ADCP traverses.

[39] Setting the zero height to $0.1D_{84}$ would be a reasonable starting point in future applications in other rivers, but preferably using local measurements of D_{84} . If most ensembles comprise many bins, our differential sensitivity argument allows the accuracy of the assumed z_0 (and thus of τ_U) to be assessed by comparing $\langle\tau_U\rangle$ with the transect average of an estimator like our τ_{u2} that uses only the lowest bin or bins that are likely to be above any effect of roughness layer distortion of the velocity profile. An independent test should ideally be made by using fixed boat ADCP measurements at several locations to obtain time-averaged velocity profiles from which to estimate z_0 by fitting the log law.

[40] The least reliable estimates by any of our methods are those for shallow channels or the shallow margins of deep channels. In shallow water the blanking distance cuts out more of the profile, the profile is defined by fewer bins so fitting the log law is even more prone to turbulent variability, and the sensitivity of τ_{u1} and τ_U to uncertainty in z_0 is greater.

[41] Agreement between ADCP-based transect-averaged shear stresses and those calculated from the depth-slope product is poor (Figure 7), but we have serious doubts about the validity of the depth-slope estimate in this river because of the strong streamwise fluctuation in water surface slope (Figure 8) and the consequent doubt about the validity of the uniform flow assumption. It would be premature to suggest on the basis of this study alone that ADCP-based estimates of mean shear stress are superior to using the depth-slope product, but we would not be surprised if this turns out to be the case once stronger tests are made of the accuracy of the ADCP methods.

[42] Our results and discussion are restricted to gravel bed rivers with high h/D_{84} ($>10^2$) and the methods which we consider promising in this context would not necessarily be

appropriate for a sand bed river with dunes or if using high-frequency ADCP in a shallow gravel bed river with obstacle clasts and $h/D_{84} < 10$.

6. Conclusions

[43] The value of moving boat ADCP surveys potentially extends beyond discharge measurement. Rapid mapping of the velocity field in a transect, at high spatial resolution, should be useful for many aspects of hydraulic and geomorphological research and habitat assessment. The main obstacle to exploiting this potential is the substantial uncertainty of the individual velocity estimates, due mainly to turbulent fluctuation at a variety of scales. This paper has explored ways to minimize the effects of this uncertainty on estimates of bed shear stress from moving boat ADCP velocity obtained at high flow from transects across a large gravel bed river. We reach the following conclusions.

[44] 1. Estimates of local shear stress can be obtained from ADCP transects by utilizing the logarithmic law of the wall, either freely fitted to each ensemble or constrained by an estimate of roughness height (in our study, based on grain size information).

[45] 2. Random noise associated with temporal flow variability, bias due to sidelobe interference and (in high flows) bed movement, and uncertainty in the exact bed elevation lead to great uncertainty in estimates of shear stress from individual velocity ensembles. The uncertainty due to turbulence depends on instrument settings and boat speed as well as the inherent characteristics of the flow. It can be reduced by averaging over adjacent ensembles before or after using the log law.

[46] 3. Comparison of smoothed estimates of shear stress for the same locations on outward and return traverses allows assessment of the precision of alternative methods of fitting the log law. We find, in agreement with *Wilcock* [1996], that using the vertically averaged mean velocity and a roughness height estimated from bed D_{84} (our τ_U) gives far more repeatable estimates than a two-parameter log-law fit (τ_{LF}), and appreciably better precision than a fit using only the lowest reliable velocity measurement and the D_{84} (τ_{u1}). This is probably because the mean velocity reflects greater averaging of turbulent fluctuations and is less affected by near-bed errors.

[47] 4. The data available to us do not allow a strong independent test of the accuracy of our methods, but we argue on mathematical grounds that the value of z_0 assumed in the methods using mean and bottom velocity must be accurate if there is 1:1 agreement between large-sample averages of shear stresses estimated using the two methods and there is a wide difference between the z/z_0 ratios. Transect-averaged shear stresses obtained by our τ_U and τ_{u2} methods do show such agreement on average, whereas τ_{u1} gives systematically slightly lower values and τ_{LF} gives generally higher but much more scattered estimates so appears to be less accurate as well as less precise. Comparison of width-averaged ADCP-based estimates of shear stress with estimates from the depth-slope product does not show good agreement, but in this river at least the use of the depth-slope product is highly suspect because of flow nonuniformity even in the flood conditions at which the ADCP measurements were made.

[48] These results are for a single reach at high discharge, and are subject to the uncertainties acknowledged above. Nevertheless they suggest that moving boat ADCP data have considerable potential for estimating transverse patterns of shear stress in large gravel bed rivers. The method using the vertically averaged velocity and a fixed roughness height appears to be fairly precise and accurate. The encouraging preliminary results in this paper suggest that further investigation is warranted.

Notation

C_d	drag coefficient (dimensionless).
D_{50}, D_{84}, D_{90}	bed grain diameters such that 50, 84, 90% are finer [L].
g	acceleration due to gravity [$L T^{-2}$], taken as 9.81 m s^{-2} .
h	local flow depth [L].
n	Manning's roughness coefficient [$L^{-1/3} T$].
S	water surface slope (dimensionless).
u	local velocity [$L T^{-1}$].
u_1	near-bed velocity.
U	vertically averaged velocity.
u^*	shear velocity.
z	height above bed [L].
z_0	height at which $u = 0$.
τ	local bed shear stress [$M L^{-1} T^{-2}$].
τ_{LF}	shear stress estimated by log-law fit.
τ_{u1}	shear stress estimated from u_1 and specified z_0 .
τ_U	shear stress estimated from U and specified z_0 .
$\langle \tau \rangle$	cross-sectionally averaged shear stress.
$\langle \tau_0 \rangle$	$\langle \tau \rangle$ based on depth-slope product.
κ	von Karman's constant (dimensionless), taken as 0.41.
ρ	water density [$M L^{-3}$], taken as 1000 kg m^{-3} .

[49] **Acknowledgments.** The ADCP data were collected by Public Works and Government Services Canada on behalf of the University of British Columbia, with funding from a Natural Science and Engineering Research Council of Canada (NSERC) strategic grant (246057; PI: M. Church) and from the British Columbia Ministry of Water, Land and Air Protection Flood Protection Program via the City of Chilliwack. R.I.F. thanks the NSERC grant and also UK Natural Environment Research Council grant NER/B/S/2002/00354 for financial support. L.C.S. began analysing the data during her Ph.D. research at the Department of Geography, University of Sheffield, which she thanks for financial support. We also thank John Pitlick and two anonymous reviewers for constructive criticisms of the first version of the paper.

References

- Biron, P. M., S. N. Lane, A. G. Roy, K. F. Bradbrook, and K. S. Richards (1998), Sensitivity of bed shear stress estimated from the vertical velocity profiles: The problem of sampling resolution, *Earth Surf. Processes Landforms*, **23**, 133–139.
- Biron, P. M., C. Robson, M. F. Lapointe, and S. J. Gaskin (2004), Comparing different methods of bed shear stress estimates in simple and complex flow fields, *Earth Surf. Processes Landforms*, **29**, 1403–1415.
- Bridge, J. S., and J. Jarvis (1977), Velocity profiles and bed shear stress over various configurations in a river bend, *Earth Surf. Processes*, **2**, 281–294.
- Dinehart, R. L., and J. R. Burau (2005), Averaged indicators of secondary flow in repeated acoustic Doppler current profiler crossings of bends, *Water Resour. Res.*, **41**, W09405, doi:10.1029/2005WR004050.
- Ellis, E. R., and M. Church (2005), Hydraulic geometry of secondary channels of lower Fraser River, British Columbia, from acoustic Doppler profiling, *Water Resour. Res.*, **41**, W08421, doi:10.1029/2004WR003777.
- Ferguson, R. I., and P. J. Ashworth (1992), Spatial patterns of bedload transport and channel change in braided and near-braided rivers, in *Dynamics of Gravel-Bed Rivers*, edited by P. Billi et al., pp. 477–496, John Wiley, Hoboken, N. J.
- Ferro, V., and G. Baiamonte (1994), Flow velocity profiles in gravel-bed rivers, *J. Hydraul. Eng.*, **120**, 60–80.
- Heathershaw, A. D. (1979), The turbulent structure of the bottom boundary layer in a tidal current, *Geophys. J. R. Astron. Soc.*, **58**, 395–430.
- Hickin, E. J. (1978), Mean flow structure in meanders of the Squamish river, British Columbia, *Can. J. Earth Sci.*, **15**, 1833–1849.
- Kostaschuk, R., P. Villard, and J. Best (2004), Measuring velocity and shear stress over dunes with acoustic Doppler profiler, *J. Hydraul. Eng. Am. Soc. Civ. Eng.*, **130**, 932–936.
- Kostaschuk, R., J. Best, P. Villard, J. Peakall, and M. Franklin (2005), Measuring flow velocity and sediment transport with an acoustic Doppler current profiler, *Geomorphology*, **68**, 25–37.
- McLean, D. G., M. Church, and B. Tassone (1999), Sediment transport along lower Fraser River: 1. Measurements and hydraulic computations, *Water Resour. Res.*, **35**, 2533–2548.
- Muste, M., K. Yu, and M. Spasojevic (2004), Practical aspects of ADCP data use for quantification of mean river flow characteristics; part I: Moving-vessel measurements, *Flow Meas. Instrum.*, **15**, 1–16.
- Nicholas, A. P. (2003), Investigation of spatially distributed braided river flows using a two-dimensional hydraulic model, *Earth Surf. Processes Landforms*, **28**, 655–674.
- Nikora, V., K. Koll, I. MacEwan, S. McLean, and A. Dittich (2004), Velocity distribution in the roughness layer of rough-bed flows, *J. Hydraul. Eng.*, **130**, 1036–1042.
- Rennie, C. D., R. G. Millar, and M. A. Church (2002), Measurement of bed load velocity using an acoustic Doppler current profiler, *J. Hydraul. Eng.*, **128**, 473–483.
- Shields, F. D., and J. R. Rigby (2005), River habitat quality from river velocities measured using acoustic Doppler current profiler, *Environ. Manage.*, **36**, 565–575.
- Smart, G. M. (1999), Turbulent velocity profiles and boundary shear in gravel bed rivers, *J. Hydraul. Eng.*, **125**, 106–116.
- Stacey, M. T., S. G. Monismith, and J. R. Burau (1999), Measurement of Reynolds stress profiles in unstratified tidal flow, *J. Geophys. Res.*, **104**, 10,933–10,949.
- Stapleton, K. R., and D. A. Huntley (1995), Seabed stress determination using the inertial dissipation method and the turbulent kinetic energy method, *Earth Surf. Processes Landforms*, **20**, 807–815.
- van Rijn, L. C. (1984), Sediment transport, part III: Bed forms and alluvial roughness, *J. Hydraul. Eng.*, **110**, 1733–1754.
- Whiting, P., and W. E. Dietrich (1991), Boundary shear stress and roughness over mobile alluvial beds, *J. Hydraul. Eng. Am. Soc. Civ. Eng.*, **116**, 1495–1511.
- Wiberg, P. L., and J. D. Smith (1991), Velocity distribution and bed roughness in high gradient streams, *Water Resour. Res.*, **27**, 825–838.
- Wilcock, P. R. (1996), Estimating local shear stress from velocity observations, *Water Resour. Res.*, **32**, 3361–3366.
- Yalin, M. S. (1992), *River Mechanics*, 220 pp., Pergamon, Oxford, U. K.
- Yorke, T. H., and K. A. Oberg (2002), Measuring river velocity and discharge with acoustic Doppler profilers, *Flow Meas. Instrum.*, **13**, 191–195.

M. Church, Department of Geography, University of British Columbia, Vancouver, BC, Canada V6T 1Z2.

R. I. Ferguson, Department of Geography, Durham University, South Road, Durham DH1 3LE, UK. (r.i.ferguson@durham.ac.uk)

L. C. Sime, British Antarctic Survey, High Cross, Madingley Road, Cambridge CB3 0ET, UK.